

Visual Tracking of Plant Virus Infection and Movement Using a Reporter MYB Transcription Factor That Activates Anthocyanin Biosynthesis^{1[W]}

Leonor C. Bedoya², Fernando Martínez², Diego Orzáez, and José-Antonio Daròs*

Instituto de Biología Molecular y Celular de Plantas (Consejo Superior de Investigaciones Científicas-Universidad Politécnica de Valencia), 46022 Valencia, Spain

Insertion of reporter genes into plant virus genomes is a common experimental strategy to research many aspects of the viral infection dynamics. Their numerous advantages make fluorescent proteins the markers of choice in most studies. However, the use of fluorescent proteins still has some limitations, such as the need of specialized material and facilities to detect the fluorescence. Here, we demonstrate a visual reporter marker system to track virus infection and movement through the plant. The reporter system is based on expression of *Antirrhinum majus* MYB-related Rosea1 (Ros1) transcription factor (220 amino acids; 25.7 kD) that activates a series of biosynthetic genes leading to accumulation of colored anthocyanins. Using two different tobacco etch potyvirus recombinant clones tagged with Ros1, we show that infected tobacco (*Nicotiana tabacum*) tissues turn bright red, demonstrating that in this context, the sole expression of Ros1 is sufficient to induce pigment accumulation to a level readily detectable to the naked eye. This marker system also reports viral load qualitatively and quantitatively by means of a very simple extraction process. The Ros1 marker remained stable within the potyvirus genome through successive infectious passages from plant to plant. The main limitation of this marker system is that color output will depend on each particular plant host-virus combination and must be previously tested. However, our experiments demonstrate accurate tracking of turnip mosaic potyvirus infecting *Arabidopsis* (*Arabidopsis thaliana*) and either tobacco mosaic virus or potato X virus infecting *Nicotiana benthamiana*, stressing the general applicability of the method.

Research in plant virology has benefited tremendously from the use of genetically encoded reporter genes (Tilsner and Oparka, 2010). Some markers, when inserted into the viral genome, report on virus infection and movement through the plant. Others, when fused to a viral gene product, report on subcellular localization of that particular viral factor. The bacterial gene coding for the enzyme GUS was used in pioneering studies (Chapman et al., 1992; Dolja et al., 1992; Scholthof et al., 1993). GUS accumulation in the plant cells in which viral expression was taking place showed the extension of infection throughout the plant. However, GUS is not a vital marker, and detection of GUS activity usually requires of destructive techniques. In contrast, the use of fluorescent protein markers as *Aequorea victoria* GFP, or any of its multiple derivatives and relatives (Day and Davidson, 2009), allows marker detection in live tissues (Baulcombe et al., 1995). Moreover combination of different fluorescent marker pro-

teins with appropriate spectral properties permits covisualization of several viral factors at the same time as well as colocalization of viral and host factors (Caplan et al., 2008; Martin et al., 2009; Wei et al., 2010a, 2010b). Techniques such as fluorescence resonance energy transfer and bimolecular fluorescence complementation, also based on the use of fluorescent proteins, reveal protein-protein interactions (Citovsky et al., 2006; Piston and Kremers, 2007; Lalonde et al., 2008). Recently, a new fluorescent marker protein (iLOV), derived from a domain of *Arabidopsis* (*Arabidopsis thaliana*) blue light receptor phototropin, was shown to offer some advantages over the GFP-derived markers as a reporter of plant virus infection and movement and when fused to proteins, mainly based on its smaller size (Chapman et al., 2008).

The current reporter technologies based on fluorescent proteins require specialized equipment for tracking viral dynamics (e.g. UV lamps), usually involving the transfer of the plants to laboratory facilities and often requiring dissecting adult plant organs for observation. This imposes limitations to the study of viral dynamics in the whole plant, particularly in field experiments or at the agronomic scale. To deal with these limitations, we propose the use of a vital visual reporter marker system based on the activation of endogenous anthocyanin biosynthetic pathways.

Anthocyanins are plant endogenous pigments with multiple roles, from adaptation to biotic and abiotic stress to cellular recycling or attraction of seed dispersers (Chalker-Scott, 1999; Ougham et al., 2005; Winfield et al., 2009). Small variations in their basic chemical composition give rise to a wide range of patterns of

¹ This work was supported by the Ministerio de Ciencia e Innovación (Spain; grant nos. BIO2008-01986 and BIO2011-26741 and also partially by grant no. BIO2010-15384) and by the Universidad Politécnica de Valencia (Spain; predoctoral fellowship to F.M.).

² These authors contributed equally to the article.

* Corresponding author; e-mail jadaros@ibmcp.upv.es.

The author responsible for distribution of materials integral to the findings presented in this article in accordance with the policy described in the Instructions for Authors (www.plantphysiol.org) is: José-Antonio Daròs (jadaros@ibmcp.upv.es).

^[W] The online version of this article contains Web-only data.

www.plantphysiol.org/cgi/doi/10.1104/pp.111.192922

light absorption, which constitutes the basis of, for example, flower colors in many species (He et al., 2011), but also provide a versatile tracking tool in plant biotechnology (Orzaez et al., 2009). The biosynthesis of anthocyanins has been extensively studied, and it is known to be activated at the transcriptional level by a triad of transcription factors, namely, an R2R3 MYB, a basic helix-loop-helix (bHLH), and a WD40 repeat protein, binding cooperatively to the promoter regions of the genes coding for the different enzymes in the pathway (Hichri et al., 2011). The overexpression of at least some of the components of the triad, usually an R2R3 MYB and a bHLH, has been used to activate anthocyanin biosynthesis (Ververidis et al., 2007). In an outstanding example, anthocyanin accumulation was induced to impressive levels in tomato (*Solanum lycopersicum*) fruits by overexpression of the garden snapdragon (*Antirrhinum majus*) transcription factors *Rosea1* (*Ros1*) and *Delila*, an R2R3 MYB, and a bHLH, respectively (Butelli et al., 2008; Luo et al., 2008).

In our previous work aimed at testing the potential use of a disarmed potyvirus-based expression vector for multigene expression in plants, we showed that coexpression of *Ros1* along with its interacting partner *Delila* induced accumulation of red anthocyanins in infected tobacco (*Nicotiana tabacum*) tissue (Bedoya et al., 2010). This result stimulated us to research the utility of these transcription factors as vital visual markers to track plant virus infection and movement through the host. Since an ideal reporter system must keep exogenous sequences to a minimum to avoid a strong influence on viral fitness, we focused on the 660-nucleotide-long open reading frame (ORF) corresponding to the snapdragon gene *Ros1*, encoding a 220-amino acid (25.7-kD) MYB-related transcription factor (Schwinn et al., 2006). Here, we show that *Ros1* is sufficient to serve as a reporter for color-based tracking of viral infection and movement in several plant virus-host combinations.

RESULTS

We constructed two recombinant *Tobacco etch virus* (TEV; genus *Potyvirus*, family *Potyviridae*) cDNAs, both including an additional cistron coding for *Ros1*. Two classic insertion positions for potyviruses were chosen (Dolja et al., 1992; Beauchemin et al., 2005; Kelloniemi et al., 2008). The first, located between P1 proteinase (P1) and helper-component proteinase (HC-Pro) cistrons, generated recombinant clone TEV-*Ros1*(P1/HC-Pro) (Fig. 1A). The second, between the RNA-dependent RNA polymerase (NIb) and the coat protein (CP) cistrons, produced recombinant clone TEV-*Ros1*(NIb/CP) (Fig. 1A). To promote the release of the heterologous protein from the viral polyprotein, in TEV-*Ros1*(P1/HC-Pro), three codons (coding for SDK) were fused to the N-terminal end of *Ros1* to complete a P1 self-proteolytic site and 11 codons (coding for TTENLYFQ/SGT) were fused to the C-terminal end of *Ros1* to introduce an NIa proteinase (NIaPro) artificial proteolytic site. In TEV-*Ros1*(NIb/CP), three codons (coding for SGT) and eight

codons (coding for TTENLYFQ) were fused to the N- and C-terminal ends, respectively, of *Ros1* to complete NIaPro-specific NIb/*Ros1* and *Ros1*/CP proteolytic sites (Supplemental Fig. S1). These cDNAs were agroinoculated in tobacco plants. New tobacco plants were mechanically inoculated with sap from infected plants in the third true leaf. For both viral recombinant clones, typical TEV symptoms arose in some of the leaves above the inoculated 4 d postinoculation (dpi). Those leaf areas first showing symptoms then turned red with an approximately 1- or 2-d delay [Fig. 1B, pictures corresponding to clone TEV-*Ros1*(NIb/CP)]. Figure 1C shows a similar time series but focusing in a single leaf, the third above the inoculated one, which showed more severe symptoms during infection. For both recombinant viruses, the pattern of red-colored anthocyanins matched exactly the pattern of TEV symptoms. Notably, symptoms and anthocyanin accumulation started in the second leaf above the inoculated, skipping one leaf, and expanded intensively up to the fourth. Further leaves showed less severe symptoms and spotty anthocyanin accumulation (Fig. 1B). To further compare the *Ros1* marker with GFP, we inoculated the third true leaf of different tobacco plants either with TEV-*Ros1*(NIb/CP) or with a TEV recombinant clone including a classic GFP marker (TEV-GFP; Fig. 1A; Supplemental Fig. S1). Fifteen days postinoculation, the visible red pattern produced by anthocyanin accumulation in plants infected by TEV-*Ros1*(NIb/CP) very much resembled the pattern of green fluorescence of plants infected by TEV-GFP (Fig. 1D), indicating that both markers display comparable outputs when reporting TEV spreading through the plant.

To further investigate if those tissues showing anthocyanin accumulation are also those supporting virus replication, we constructed an additional recombinant TEV cDNA including two marker cistrons: GFP was inserted between P1 and HC-Pro and *Ros1* between NIb and CP (Fig. 2A). The N- and C-terminal peptides described above were fused to both markers to assure proper release from the viral polyprotein (Supplemental Fig. S1). The viral cDNA was agroinoculated in tobacco plants, and symptomatic leaves were inspected at several days postinoculation. GFP fluorescence was detected in leaves above the agroinoculated, concurrently to symptom development. Anthocyanin accumulation was detected in exactly the same tissues with an approximately 2-d delay. Figure 2B shows a sector of an infected tobacco leaf (8 dpi) with a matching reticulate pattern of green fluorescence and visible red color. Figure 2C shows a whole infected plant (8 dpi) with matching patterns of green fluorescence produced by GFP and red visible coloration resulting from anthocyanin accumulation. This demonstrates that the tissues in which the red-colored anthocyanins are visually detected are those in which viral genome is being expressed. The delay observed between the fluorescent detection of GFP and the visual detection of anthocyanins suggests that *Ros1* needs some time to exert its regulatory action, which nevertheless culminates with pigment accumulation reaching levels sufficient for simple visual detection.

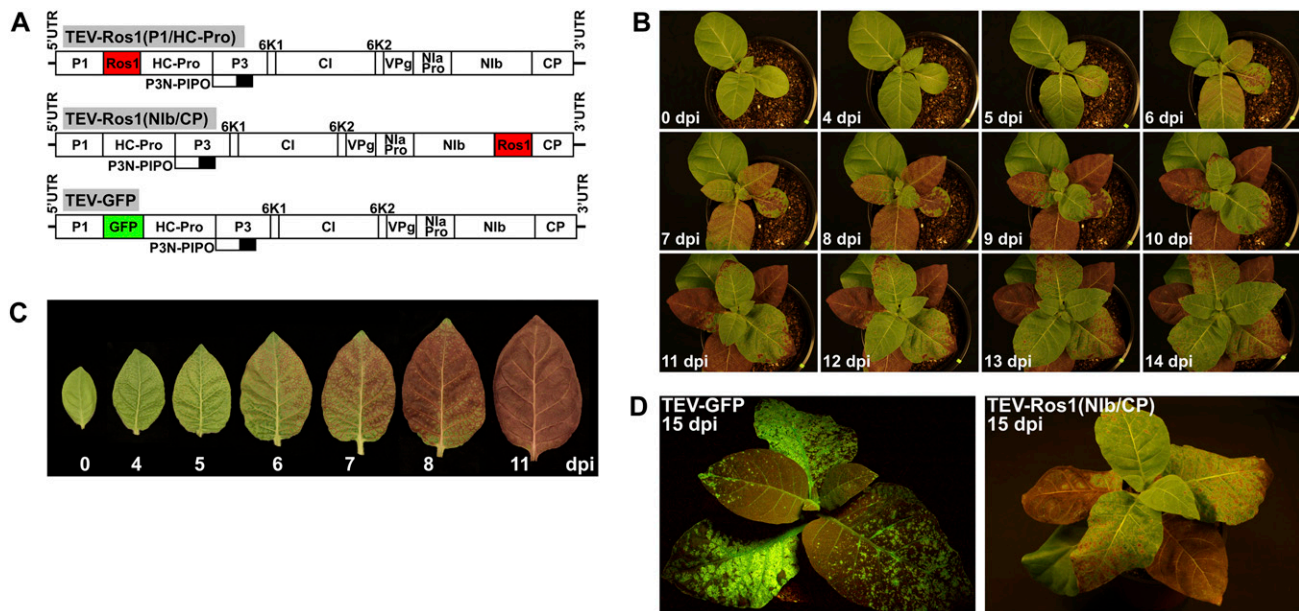


Figure 1. Anthocyanin accumulation in tobacco plants infected by recombinant TEV clones that include the transcription factor Ros1 as a vital visual marker. A, Schematic representation of recombinant clones TEV-Ros1(P1/Hc-Pro), TEV-Ros1(Nib/CP), and TEV-GFP. TEV 5' and 3' untranslated regions (UTRs) are indicated by lines; TEV cistrons P1, HC-Pro, P3, P3N-PIPO, 6K1, CI, 6K2, VPg, NlaPro, Nib, and CP by boxes; and Ros1 and GFP cistrons by green and red boxes, respectively. B, Pictures at various days postinoculation of a tobacco plant inoculated with TEV-Ros1(Nib/CP). C, Pictures at various days postinoculation of the third leaf above the inoculated from tobacco plants infected with TEV-Ros1(Nib/CP). D, Pictures at 15 dpi of two different tobacco plants inoculated with TEV-GFP (taken with a yellow filter under UV illumination) and TEV-Ros1(Nib/CP).

To confirm the apparent correlation between virus replication and pigment accumulation, we infected tobacco plants with TEV-Ros1(Nib/CP) and harvested the second leaf above the inoculated at 9 dpi. This leaf typically develops symptoms only in the basal part. Tissue was sampled and RNA purified from the green and red parts of the leaf, as well as in the border between both regions (Fig. 3A). In the analysis, a control from a noninoculated plant was also included. Next, the presence of TEV was detected by reverse transcription (RT)-PCR. A 790-bp TEV-specific DNA was exclusively amplified from the tissues in the red and green-red border part of the leaf (Fig. 3B, lanes 3 and 4), indicating that TEV genome is only substantially present in those tissues that accumulated anthocyanins.

We then asked if the amount of anthocyanin accumulating in infected tissue quantitatively correlated to viral load. To address this question, we recurred to three TEV mutant clones showing defects in viral accumulation compared to the wild type. TEV-CLA2, TEV-AS13a, and TEV-AS20a contain mutations in the allele corresponding to the viral RNA silencing suppressor HC-Pro. These mutations confer RNA silencing hyposuppressor activity to the corresponding proteins, resulting in lower viral genome amplification capacity during protoplast infection and a lower viral load in infected plants (Kasschau et al., 1997; Torres-Barceló et al., 2008, 2010). Note that AS13a and AS20a contain only one of the two mutations present in the previously described hyposuppressor mutants AS13 and AS20 (Kasschau et al., 1997; Torres-

Barceló et al., 2008). Mutations were transferred to TEV-Ros1(Nib/CP) cDNA, creating TEV(CLA2)-Ros1(Nib/CP), TEV(AS13a)-Ros1(Nib/CP), and TEV(AS20a)-Ros1(Nib/CP). These cDNAs, as well as the corresponding wild-type control TEV-Ros1(Nib/CP), were agroinoculated in tobacco plants, and virions were purified from infected tissue. Virion concentration in each preparation was quantified by western analysis using an antibody against CP. Subsequently, tobacco plants were mechanically inoculated with normalized amounts of the different virion preparations. During the following days, red coloration appeared in all infected plants, but those infected with TEV mutants showed lower pigmentation than those infected with the wild-type control. Figure 4A depicts the third leaves above those inoculated taken from representative plants at 10 dpi. Tissue from these third leaves was harvested from three independent plants infected with each virion preparation, as well as from a noninoculated control. In those tissues, viral load was quantified by western analysis using the anti-CP antibody. Anthocyanins were also extracted from the same tissues and quantified spectrophotometrically. The plot in Figure 4B shows a good correlation between anthocyanin accumulation and viral load. These results indicate that Ros1 readily reports on viral load both qualitatively (eye inspection) but also quantitatively through a very simple colorimetric assay of a tissue homogenate.

To further research the correlation between virus and anthocyanin accumulations, we infected a series of to-

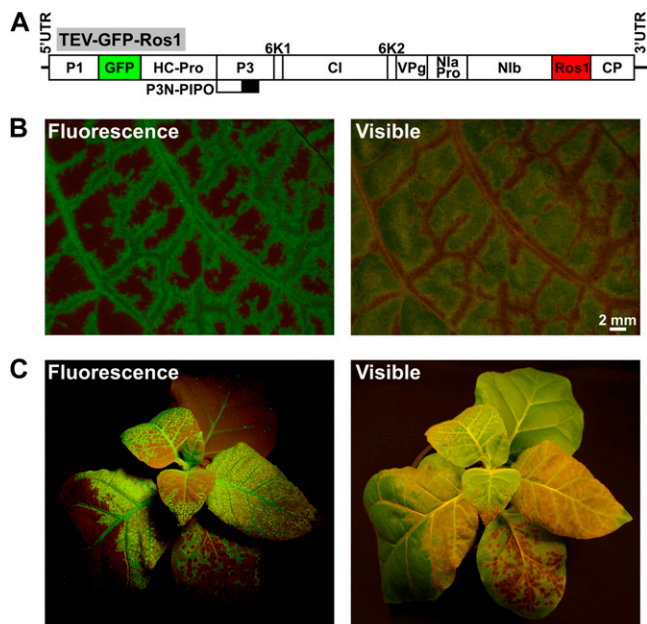


Figure 2. Green fluorescence and anthocyanin accumulation in a tobacco plant infected by a recombinant TEV clone that includes GFP and Ros1 reporter markers. A, Schematic representation of the recombinant clone TEV-GFP-Ros1. GFP and Ros1 cistrons are represented by green and red boxes, respectively. Other details are as in Figure 1A; UTR, untranslated region. B, Stereomicroscope pictures of an infected tobacco leaf under green fluorescence and visible conditions. Bar = 2 mm. C, Pictures of the whole plant at 8 dpi taken under UV illumination with a yellow filter and under regular white light.

...bacco plants with TEV-Ros1(NIb/CP) in the third true leaf and harvested the third leaves above the inoculated at different days postinoculation. From each leaf, two comparable tissue aliquots were used to simultaneously analyze virus CP accumulation by western blot and anthocyanin accumulation spectrophotometrically (Fig. 4C). The plot in Figure 4D shows that viral load increases with time after 4 dpi, reaching a maximum at 8 dpi and then decreasing. The time course of anthocyanin accumulation follows the same tendency with an about 2-d delay.

To perform properly as a reporter of plant virus infection, Ros1 should be maintained in the recombinant virus genome for the whole infectious cycle. To analyze this question, a virus inoculum from an initially agro-inoculated tobacco plant was serially propagated from plant to plant each 9 d. Pictures of the successive infected plants were taken just before harvesting the tissue for the subsequent passage (Fig. 5). This experiment spanned a total of six passages (seven infected plants) and demonstrates the high stability of the Ros1 reporter in the TEV genome.

Finally, we tested if the reporter properties shown by Ros1 in infections of tobacco by TEV can be extended to other viruses belonging to the same or different taxonomic groups and to different host plant species. Toward this aim, we constructed additional recombinant viral cDNAs including the Ros1 reporter marker. Ros1 was inserted between NIb and CP in a *Turnip mosaic virus* (TuMV; genus *Potyvirus*, family *Potyviridae*) infectious cDNA (TuMV-Ros1; Fig. 6A). Ros1 included N- and C-terminal peptide fusions to complete TuMV NIaPro cleavage sites NIb/Ros1 and Ros1/CP (Supplemental Fig. S1). Ros1 was also inserted after a duplicated CP promoter in the cDNAs of *Tobacco mosaic virus* (TMV; genus *Tobamovirus*, family *Virgaviridae*), of *Potato virus X* (PVX; genus *Potexvirus*, family *Alphaflexiviridae*), and of the RNA 2 of *Tobacco rattle virus* (TRV; genus *Tobravirus*, family *Virgaviridae*) to create TMV-Ros1, PVX-Ros1, and TRV2-Ros1, respectively (Fig. 6A). The full sequences of all these virus recombinant cDNAs are in Supplemental Figure S1.

First, the model plant *Arabidopsis* (accession Columbia-0) was mechanically inoculated with inocula containing either wild-type TuMV or TuMV-Ros1. Inoculated plants developed the symptoms characteristic of TuMV. Again with some delay, symptomatic tissue became purple, indicating anthocyanin accumulation. Figure 6B shows representative *Arabidopsis* plants infected by wild-type TuMV and TuMV-Ros1 at 20 dpi. The purple color is particularly visible on the reverse side of the leaves. Second, *Nicotiana benthamiana* plants, also a model in many studies in plant virology, were inoculated mechanically with

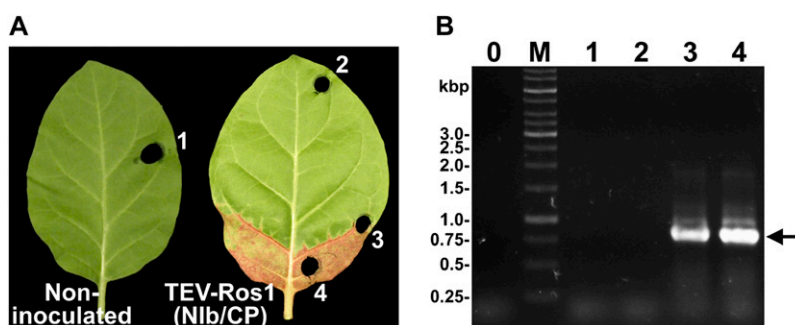


Figure 3. TEV diagnosis in a tobacco leaf infected by TEV-Ros1(NIb/CP). A, RNA was extracted and purified from tissue samples from a tobacco noninoculated control (1) and from a tobacco leaf infected by TEV-Ros1(NIb/CP) showing green (2), green-red (3), or red (4) pigmentation. B, TEV was diagnosed by RT-PCR and the amplification products separated by agarose electrophoresis. Lane 0, RT-PCR negative control with no template; lane M, DNA ladder markers with some sizes indicated on the left; lanes 1 to 4, RT-PCR products amplified from RNA samples 1 to 4. The 790-bp TEV-specific DNA amplification product corresponding to CP cistron is indicated by an arrow.

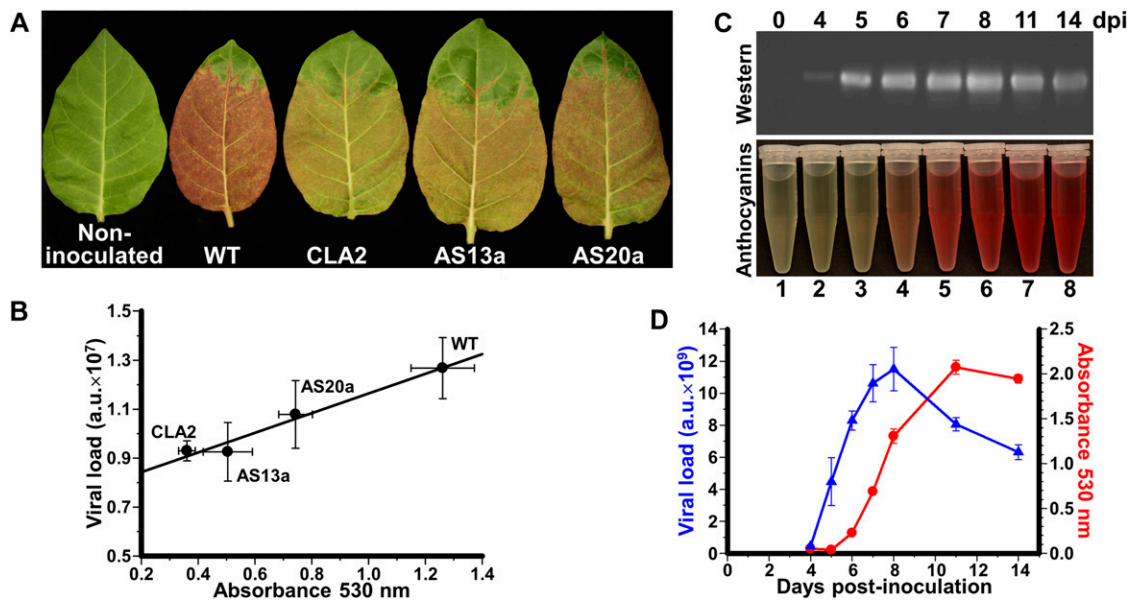


Figure 4. Correlation between anthocyanin accumulation and viral load in tobacco leaves infected by TEV-Ros1(NiB/CP) and the corresponding HC-Pro mutants CLA2, AS13a, and AS20a. A, Pictures of the third leaves above the inoculated from tobacco plants noninoculated or infected (10 dpi) with TEV-Ros1(NiB/CP) (WT), TEV(CLA2)-Ros1(NiB/CP) (CLA2), TEV(AS13a)-Ros1(NiB/CP) (AS13a), and TEV(AS20a)-Ros1(NiB/CP) (AS20a). B, Plot of the viral load (measured as the accumulation of the virus CP by western blot in arbitrary units [a.u.]) versus anthocyanin accumulation (A_{530}) in triplicate plants infected by TEV-Ros1(NiB/CP) (WT), CLA2, AS13a, and AS20a mutants. Bars indicate the SE of each measure. A regression line was fitted to the data ($y = 0.4x + 0.76$, $r = 0.98$). C, Western-blot analysis of TEV CP and anthocyanin accumulation in the third leaves above the inoculated of tobacco plants infected by TEV-Ros1(NiB/CP) at 0, 4, 5, 6, 7, 8, 11, and 14 dpi (lanes 1–8). D, Plots of viral load (blue triangles) and anthocyanin accumulation (red circles) in the third leaves above the inoculated versus days postinoculation in tobacco plants inoculated with TEV-Ros1(NiB/CP). Bars indicate the SE of the measures in triplicate plants.

inocula corresponding to TEV-Ros1(NiB/CP), TMV-Ros1, PVX-Ros1, and TRV-Ros1 (containing TRV1 and TRV2-Ros1). Inocula originated from previously agroinoculated plants. Between 8 and 13 dpi, the different viruses had induced their characteristic symptoms. With an approximately 2-d delay, symptomatic tissue became brown in the case of TEV-Ros1(NiB/CP), TMV-Ros1, and PVX-Ros1 (Fig. 6C). Although TRV-Ros1 induced symptoms, symptomatic tissue never developed any pigmentation that could be attributed to anthocyanin accumulation (Fig. 6C).

DISCUSSION

Here, we show the use of natural plant pigments as a reporter system for visual tracking of plant virus infection dynamics through the plant. The system is based on the expression of the MYB-related snapdragon transcription factor Ros1, which activates anthocyanin biosynthesis. There are a few examples in the literature in which plant pigments are used as visual reporter systems, most of them consisting of tissue depigmentation. The silencing of phytoene desaturase, a gene involved in carotenoid biosynthesis, is often used as a marker of virus-induced gene silencing. The lack of carotenoids destabilizes the chlorophylls, yielding a readily visible white phenotype (Liu et al., 2002). Silencing of phytoene desaturase also served as reporter in such carotenoid-

rich organs as tomato fruits (Fu et al., 2005; Orzaez et al., 2006). Similarly, silencing of chalcone synthase, a key enzyme in anthocyanin biosynthesis, has been used as an endogenous reporter for gene silencing in such anthocyanin-rich organs as flower petals (Chen et al., 2004). Silencing of the transgenically expressed transcription factors Ros1 and Delila was also used as a virus-induced gene silencing reporter in purple tomatoes (Orzaez et al., 2009). In contrast, strategies based on induction of tissue pigmentation are not so common, although recently, anthocyanin accumulation has been proposed as a method for identity preservation in plant biotechnology (Juárez et al., 2011) and as a selection system in plant transformation (Kortstee et al., 2011).

The experiments shown here demonstrate that the snapdragon transcription factor Ros1 may be useful as a reporter gene in the research of many aspects of plant molecular virology and virus-plant interaction for a series of virus-host plant combinations. Ros1 interacts with the companion transcription factor Delila to activate almost all genes encoding anthocyanin biosynthetic enzymes, including genes required for side chain modification and two genes involved in vacuolar import (Schwinn et al., 2006; Butelli et al., 2008). Previously, we showed that the simultaneous expression of both transcription factors Delila and Ros1 through a disarmed TEV-based expression vector induced a dark red coloration in infected tobacco tissues (Bedoya et al.,

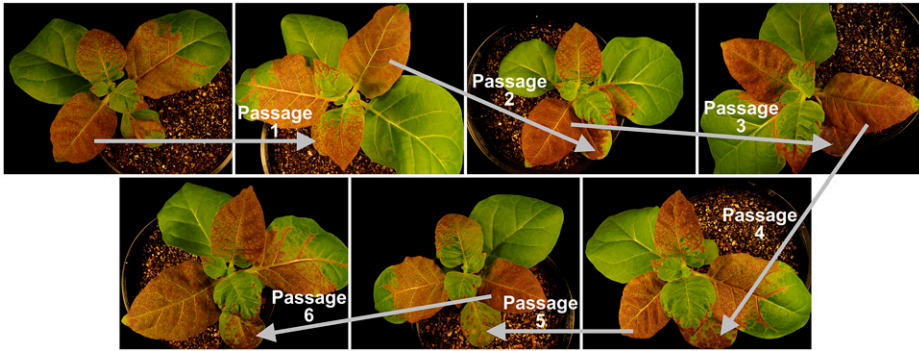


Figure 5. Stability of the Ros1 reporter marker in TEV-Ros1(NIb/CP) through six infective passages in tobacco plants. The first plant was agroinoculated and the following were successively inoculated with sap from the previous infected plant. Pictures were taken at 9 dpi just before passaging.

2010). However, the combined size of Delila and Ros1 cDNAs (2592 bp) precludes the use of both proteins as a reporter marker system. In this work, we show that the sole expression of Ros1 is sufficient to induce anthocyanin accumulation to a level clearly visible to the naked eye (Fig. 1). The *Ros1* ORF is 660 bp and codes for a 25.7-kD protein. This size is comparable to those of GFP and related fluorescent proteins. However, it is significantly larger than the approximately 10-kD fluorescent reporter iLOV (Chapman et al., 2008). Nonetheless, as a clear advantage of Ros1 versus GFP or iLOV, the product of Ros1 activity (anthocyanins) can be easily detected by the

naked eye. Consequently, many plants could be quickly monitored and screened visually without the need for artificial irradiation and in a nondestructive manner. This property may be desirable in experimental strategies in which plant viruses are used for large screenings or in which virus properties like infectivity or systemic movement are screened in many virus mutants. A disadvantage of Ros1 is that the visual detection of anthocyanins is delayed about 2 d when compared to detection of GFP fluorescence, and this could be a limitation for some experimental setups in which a precise time course of virus infection dynamics is needed. The suitability of a reporter

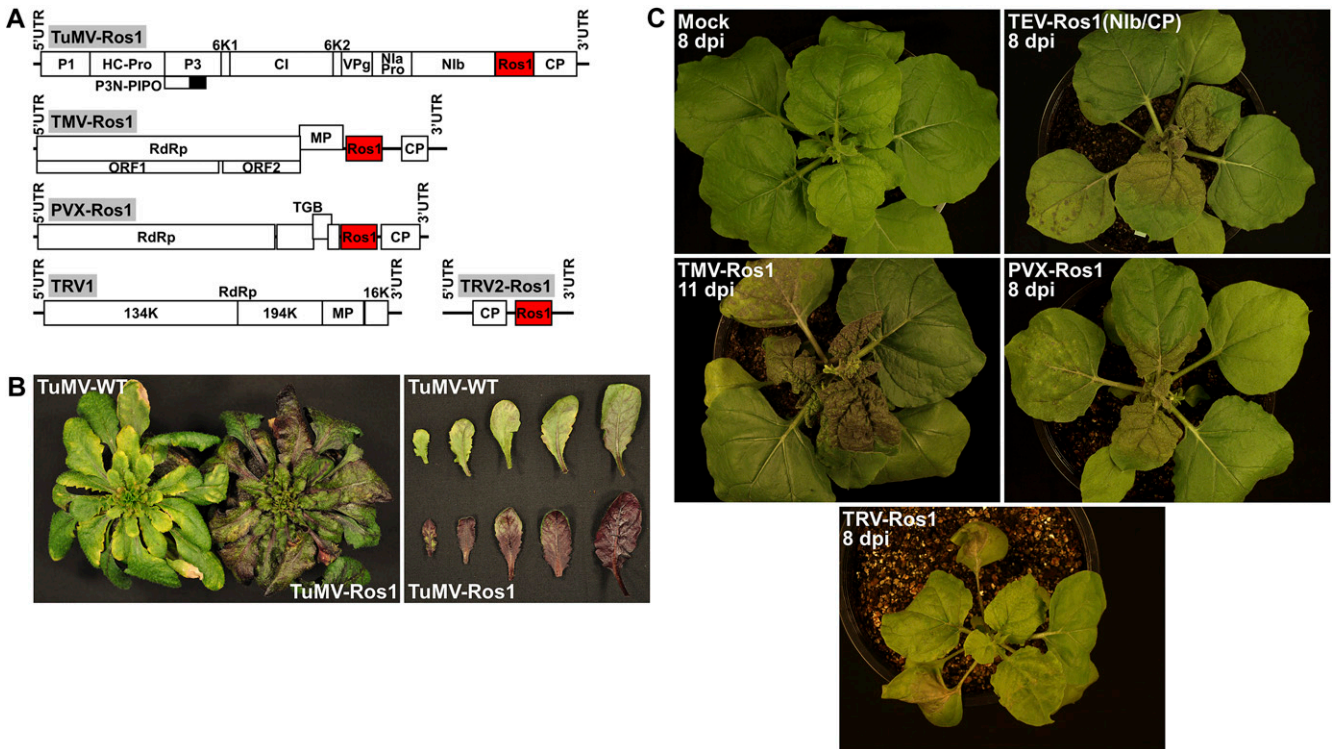


Figure 6. Anthocyanin accumulation in *Arabidopsis* and *N. benthamiana* plants infected by recombinant clones of several viruses, including the Ros1 reporter marker. A, Schematic representation of TuMV-Ros1, TMV-Ros1, PVX-Ros1, TRV1, and TRV2-Ros1. Ros1 marker is represented by a red box. RNA-dependent RNA polymerases (RdRp), movement proteins (MP), and triple gene block (TGB) are represented by boxes. Other details are as in Figure 1A; UTR, untranslated region. B, Pictures of *Arabidopsis* plants infected by TuMV-WT and TuMV-Ros1 (20 dpi). A detail of the reverse side of the leaves is also included. C, Pictures of *N. benthamiana* plants mock inoculated and infected by TEV-Ros1(NIb/CP), TMV-Ros1, PVX-Ros1, and TRV-Ros1 at different days postinoculation.

system of this kind, based on the production of anthocyanin pigments as a way to noninvasively identify an infected cell, was already discussed when Baulcombe et al. (1995) demonstrated the properties of GFP as a reporter for virus infection.

The success of a virus-encoded R2R3 MYB transcription factor at inducing anthocyanin accumulation in the absence of its interaction partners is not entirely surprising. It has been observed before that the MYB component is often the limiting factor in anthocyanin production (Piazza et al., 2002; Schwinn et al., 2006; Albert et al., 2011). The sole overexpression of some R2R3 MYB factors like tomato ANT1 or petunia (*Petunia × hybrida*) DPL and PHZ induced red or purple coloration in vegetative tissues (Mathews et al., 2003; Albert et al., 2011). However, the overexpression of the MYB component is not always sufficient. Transient expression of an apple (*Malus × domestica*) MYB factor (MdMYB10) induced only a weak anthocyanin response in *N. benthamiana* and required the presence of a recombinant bHLH partner to fully activate the target promoters (Espley et al., 2007; Lin-Wang et al., 2010). In our case, the expression levels conferred by the different viruses or the concomitant expression of the corresponding viral RNA silencing suppressors may explain the ability of Ros1 to activate pigmentation on its own in most instances. Moreover, its endogenous interaction partners could themselves be activated by the stress imposed by the virus infection, resulting in an enhanced anthocyanin response. Indeed, it is known that viral infection can activate anthocyanin biosynthesis (Gutha et al., 2010); therefore, we cannot discard that the suitability of Ros1 as a minimal reporter for viral infection in different host species is partially the consequence of the activation of its endogenous interaction partners as a result of the infection. In this sense, the complementation in trans with additional factors, like Delila (introduced as a stable transgene), could be used in the future as a way to modulate the output signal. More elaborated strategies may include the expression of engineered targets of the transcription factor coding for different anthocyanin biosynthetic enzymes as a way to modulate color outputs.

In the potyviruses TEV and TuMV, Ros1 is expressed as part of the viral polyprotein, which is subsequently processed by the viral-encoded proteases. Once released from the viral polyprotein, Ros1 must move to the nucleus to induce anthocyanin biosynthesis. The need for nuclear traffic imposes a limitation to this marker when compared with others like GFP or iLOV, whose intrinsic fluorescence is directly detected. While GFP and iLOV can be used as reporters either as free proteins or when fused to viral proteins, translational fusion of Ros1 to a viral protein may interfere with its regulatory activity. However, the Ros1-based reporter system relying on enzymatic synthesis of pigments may offer increased sensitivity with respect to fluorescent protein markers, similarly to the GUS system, but without the major drawback of destructive sampling.

Our experiments also demonstrated an exquisite colocalization between pigment accumulation and the pres-

ence of the Ros1-tagged TEV. This is deduced from the matching patterns of green fluorescence and red pigmentation in tobacco leaves infected by the doubly tagged TEV-GFP-Ros1 (Fig. 2) and from the amplification by RT-PCR of a specific TEV cDNA exclusively from those parts of an infected leaf showing the red pigmentation (Fig. 3). These results suggest that the anthocyanin biosynthetic induction triggered by Ros1 expression is cell autonomous and does not extend to neighboring tissues or even to the whole plant. This property enables the use of Ros1 to track the virus movement through the plant to study which tissues are invaded by the virus and which are not and to accurately dissect viral and host factors involved in virus cell-to-cell and systemic movement.

In fact, direct observation of tobacco plants infected by TEV-Ros1(NIb/CP) suggests that, when inoculated in the third true leaf, the virus skips the next leaf, colonizes the basal half of the subsequent one, and completely colonizes the third and fourth leaves above the inoculated and only patches of more distal leaves (Fig. 1B). At the end, there are new leaves growing that are apparently free of the virus. This observation is coherent with a burst of virus replication and movement during the first days after infection that is finally controlled or ameliorated by the plant antiviral defenses. Nonetheless, we cannot discard the potential presence of minimal amounts of TEV particles in non-red tissues either not expressing the viral genome or expressing it in an amount insufficient to trigger visible anthocyanin accumulation. The infection dynamics of TEV-Ros1(NIb/CP) and TEV-GFP are very similar (Fig. 1D), indicating that the Ros1 marker has no more impact on virus fitness than GFP.

In addition, our experiments also show that Ros1 is a quantitative reporter because anthocyanin accumulation correlates viral load (Fig. 4). Precise quantification can be performed by a very cheap and simple extraction process with acidified methanol followed by a colorimetric measurement (see "Materials and Methods"). In any case, visual inspection of infected tissues gives a qualitative idea of virus accumulation that can be sufficient for many purposes (Fig. 4, A and C). Also of importance is the high stability of Ros1 in the genome of the recombinant TEV during the infectious cycle and through successive passages from plant to plant (Fig. 5). Nonetheless, this property is expected to depend on the particular virus species, since some viruses accept insertions better than others. Also, stability will depend on the particular constructive details of each recombinant virus cDNA clone. In our TEV constructs, attention has been paid to avoid long sequence repetitions when inserting the Ros1 marker to avoid undesired homologous recombination (Supplemental Fig. S1).

Finally, our experiments also demonstrate that the properties of Ros1 as a reporter marker can be extended to other viruses belonging to different taxonomic groups and other host plants (Fig. 6). However, this property is not universal, as exemplified by the case of TRV-Ros1 infecting *N. benthamiana*. Since Ros1 needs to move to the nucleus to act and since each particular plant species

or plant taxonomic group has a particular anthocyanin biosynthetic pathway, it is expected that the performance of Ros1 as a reporter marker will depend on each particular virus-host combination. In our work, best results were obtained with TEV-infecting tobacco plants, in which Ros1 produces an intense bright red pigmentation (Fig. 1). Good results were also obtained with TuMV infecting Arabidopsis plants. In this case, the purple pigmentation was particularly bright on the reverse side of the leaves (Fig. 6B). Finally, *N. benthamiana* developed a less bright, although clearly visible, brown coloration with TEV, TMV, and PVX (Fig. 6C). These differences in accumulation and color may reflect the complex interaction of Ros1 with its endogenous partners, giving rise to the transcriptional activation of different enzymes in different plant species. Additionally, phenotypic differences between species may also be due to the different redox status of the vacuolar milieu. In conclusion, despite these drawbacks, Ros1 promises to be a useful vital visual marker to track virus infection and movement and to easily quantify viral load for many virus-plant host combinations.

MATERIALS AND METHODS

Plasmids

Virus clones TEV-Ros1(P1/HC-Pro), TEV-Ros1(NIb/CP), TEV-GFP, TEV-GFP-Ros1, TuMV-WT, TuMV-Ros1, TMV-Ros1, and PVX-Ros1 were produced from plasmids pGTEV-Ros1(P1/HC-Pro), pGTEV-Ros1(NIb/CP), pGTEV-GFP, pGTEV-GFP-Ros1, pTuMV, pTuMV-Ros1, pTMV-Ros1, and pPVX-Ros1, respectively. Virus clone TRV-Ros1 was produced from plasmids pTRV1 (Liu et al., 2002) and pTRV2-Ros1. Plasmid pGTEV_a derives from pGTEV (Bedoya and Daròs, 2010) and contains the TEV cDNA corresponding to GenBank accession number DQ986288 under the control of *Cauliflower mosaic virus* 35S promoter and terminator, but includes two silent mutations (G273A and A1119G) to remove internal *BsaI* restriction sites. In pGTEV-Ros1(P1/HC-Pro), pGTEV-Ros1(NIb/CP), pGTEV-GFP, and pGTEV-GFP-Ros1, the Ros1 (DQ275529) and the enhanced GFP (AAB08060) cDNAs were inserted in different positions of pGTEV_a by standard techniques based on the use of the type IIIs restriction enzyme *BsaI* (New England Biolabs) and T4 DNA ligase (Fermentas; Engler et al., 2009). The complete sequences of the resulting viral cDNAs contained in those plasmids are in Supplemental Figure S1. pGTEV(CLA2)-Ros1(NIb/CP), pGTEV(AS13a)-Ros1(NIb/CP), and pGTEV(AS20a)-Ros1(NIb/CP) were like pGTEV-Ros1(NIb/CP) but included the mutations T1631C (CLA2), A1952C (AS13a), or A2135C (AS20a) in the TEV cDNA (HC-Pro cistron). pTuMV-Ros1 is like pTuMV-GFP (Martínez et al., 2011), but replacing the GFP between NIb and CP by Ros1 (Supplemental Fig. S1). In pTMV-Ros1, Ros1 cDNA replaces dsRed of pTMV-dsRed (Canto and Palukaitis, 2002). In pPVX-Ros1, Ros1 cDNA is inserted after the duplicated CP promoter of pGR107 (Lu et al., 2003). In pTRV2-Ros1, Ros1 cDNA replaces a region in the virus genome from position 1344 to 1694 of AF406991, including both 28.7K and 32.8K ORFs (Liu et al., 2002). The full sequences of the viral cDNAs in all these plasmids are in Supplemental Figure S1.

Plant Inoculation

For agroinoculation of TEV-Ros1(P1/HC-Pro), TEV-Ros1(NIb/CP), TEV-GFP, TEV-GFP-Ros1, and PVX-Ros1, *Agrobacterium tumefaciens* C58C1 containing the helper plasmid pCLEAN-S48 (Thole et al., 2007) was transformed with the corresponding plasmids (see above). Bacteria were grown in liquid culture, adjusted at 0.5 OD₆₀₀ in induction buffer (10 mM MES-NaOH, pH 5.6, 10 mM MgCl₂, and 150 μM acetosyringone), cultured for 2 h at 28°C, and infiltrated in a plant leaf (Bedoya and Daròs, 2010). For agroinoculation of TRV-Ros1, two cultures of *A. tumefaciens* C58C1 each transformed with pTRV1 or pTRV2-Ros1 were treated as above, mixed, and infiltrated. TuMV-WT and TuMV-Ros1 were mechanically inoculated from plasmids pTuMV (Martínez et al., 2011) and pTuMV-Ros1. Finally, TMV-Ros1 was mechanically inoculated from 5'-capped RNA transcripts obtained

by in vitro transcription (Bedoya and Daròs, 2010) with T7 RNA polymerase (Epicentre) of plasmid pTMV-Ros1 digested by *KpnI* (Fermentas).

Plants were also mechanically inoculated with sap from a previously infected plant. Approximately 100 mg of frozen tissue was homogenized in 20 volumes of inoculation buffer (50 mM potassium phosphate, pH 8.0, 1% polyvinylpyrrolidone 10, 1% polyethylene glycol 6000, and 10 mM 2-mercaptoethanol). A cotton swab was soaked in the plant homogenate and gently rubbed on a leaf in which two 10-μL drops of 10% carborundum in inoculation buffer were previously deposited (Bedoya et al., 2010).

Nicotiana tabacum and *Nicotiana benthamiana* plants were grown in a greenhouse at 25°C with a 16-h-day/8-h-night cycle. When inoculated, plants were transferred to a growth chamber with a 12-h-day/12-h-night and 25°C/23°C cycle. Arabidopsis (*Arabidopsis thaliana*) plants were grown all the time in these last conditions.

TEV Diagnosis by RT-PCR

RNA was purified from frozen tissue using silica gel columns and eluted in 10 μL (Zymo Research). One microliter of RNA was subjected to reverse transcription with M-MuLV reverse transcriptase (Fermentas) using primer I (5'-CTCGCACTA-CATAGGAGAATTAGAC-3') in a 10-μL volume reaction and 1 μL of this reaction was subjected to PCR amplification with *Thermus thermophilus* DNA polymerase (Biotools) with primers II (5'-AGTGGCACTGTGGGTGCTGGTGTG-3') and III (5'-CTGGCGGACCCCTAATAG-3') in a 20-μL volume reaction. Reaction conditions were as previously described (Bedoya et al., 2010). PCR products were analyzed by electrophoresis in 1% agarose gels in TAE buffer (40 mM Tris, 20 mM sodium acetate, and 1 mM EDTA, pH 7.2) and staining with ethidium bromide.

Western Analysis

Frozen tissue (around 120 mg) was homogenized in 3 volumes of TEW (60 mM Tris-HCl, pH 6.8, 2% SDS, 100 mM dithiothreitol, 10% glycerol, and 0.01% bromophenol blue). The extract was heated for 5 min at 98°C, vortexed, and clarified by centrifugation. Supernatants (5 μL) were separated by discontinuous PAGE in the presence of SDS (SDS-PAGE) in 12.5% polyacrylamide (resolving gel). Proteins were electroblotted to a polyvinylidene difluoride membrane (GE Healthcare) and TEV CP detected through an overnight incubation at room temperature with a 1:10,000 dilution of an anti-CP polyclonal antibody conjugated to alkaline phosphatase (Agdia; Bedoya et al., 2010). Alkaline phosphatase was detected using a chemiluminescent substrate (CSPD; Roche) and quantified with a luminescent image analyzer (LAS-3000; Fujifilm).

Anthocyanin Quantification

Frozen tobacco tissue (around 150 mg) was homogenized in 50 volumes of extraction solution (0.037% HCl in methanol). The extract was vortexed vigorously, incubated for 1 h on ice, and clarified by centrifugation for 5 min at 13,000g. Anthocyanin concentration was measured in the supernatant quantifying A₅₃₀ and subtracting the absorbance of a similar extract from a noninoculated plant.

Supplemental Data

The following materials are available in the online version of this article.

Supplemental Figure S1. Full sequence of the recombinant viral clones TEV-Ros1(P1/HC-Pro), TEV-Ros1(NIb/CP), TEV-GFP, TEV-GFP-Ros1, TuMV-Ros1, TMV-Ros1, PVX-Ros1, and TRV2-Ros1.

ACKNOWLEDGMENTS

We thank Verónica Aragónés (Instituto de Biología Molecular y Celular de Plantas, Consejo Superior de Investigaciones Científicas-Universidad Politécnica de Valencia, Valencia, Spain) for excellent technical assistance and C. Douglas Grubb (Leibniz-Institut für Pflanzenbiochemie, Germany) for critical review of the manuscript.

Received December 28, 2011; accepted January 11, 2012; published January 11, 2012.

LITERATURE CITED

Albert NW, Lewis DH, Zhang H, Schwinn KE, Jameson PE, Davies KM (2011) Members of an R2R3-MYB transcription factor family in *Petunia*

- are developmentally and environmentally regulated to control complex floral and vegetative pigmentation patterning. *Plant J* **65**: 771–784
- Baulcombe DC, Chapman S, Santa Cruz S** (1995) Jellyfish green fluorescent protein as a reporter for virus infections. *Plant J* **7**: 1045–1053
- Beauchemin C, Bougie V, Laliberté JF** (2005) Simultaneous production of two foreign proteins from a polyvirus-based vector. *Virus Res* **112**: 1–8
- Bedoya L, Martínez F, Rubio L, Daròs JA** (2010) Simultaneous equimolar expression of multiple proteins in plants from a disarmed potyvirus vector. *J Biotechnol* **150**: 268–275
- Bedoya LC, Daròs JA** (2010) Stability of *Tobacco etch virus* infectious clones in plasmid vectors. *Virus Res* **149**: 234–240
- Butelli E, Titta L, Giorgio M, Mock HP, Matros A, Peterek S, Schijlen EG, Hall RD, Bovy AG, Luo J, et al** (2008) Enrichment of tomato fruit with health-promoting anthocyanins by expression of select transcription factors. *Nat Biotechnol* **26**: 1301–1308
- Canto T, Palukaitis P** (2002) Novel N gene-associated, temperature-independent resistance to the movement of tobacco mosaic virus vectors neutralized by a cucumber mosaic virus RNA1 transgene. *J Virol* **76**: 12908–12916
- Caplan JL, Mamillapalli P, Burch-Smith TM, Czymmek K, Dinesh-Kumar SP** (2008) Chloroplastic protein NRIP1 mediates innate immune receptor recognition of a viral effector. *Cell* **132**: 449–462
- Citovsky V, Lee LY, Vyas S, Glick E, Chen MH, Vainstein A, Gafni Y, Gelvin SB, Ztfira T** (2006) Subcellular localization of interacting proteins by bimolecular fluorescence complementation *in planta*. *J Mol Biol* **362**: 1120–1131
- Chalker-Scott L** (1999) Environmental significance of anthocyanins in plant stress responses. *Photochem Photobiol* **70**: 1–9
- Chapman S, Faulkner C, Kaiserli E, Garcia-Mata C, Savenkov EI, Roberts AG, Oparka KJ, Christie JM** (2008) The photoreversible fluorescent protein iLOV outperforms GFP as a reporter of plant virus infection. *Proc Natl Acad Sci USA* **105**: 20038–20043
- Chapman S, Kavanagh T, Baulcombe D** (1992) Potato virus X as a vector for gene expression in plants. *Plant J* **2**: 549–557
- Chen JC, Jiang CZ, Gookin TE, Hunter DA, Clark DG, Reid MS** (2004) Chalcone synthase as a reporter in virus-induced gene silencing studies of flower senescence. *Plant Mol Biol* **55**: 521–530
- Day RN, Davidson MW** (2009) The fluorescent protein palette: tools for cellular imaging. *Chem Soc Rev* **38**: 2887–2921
- Dolja VV, McBride HJ, Carrington JC** (1992) Tagging of plant potyvirus replication and movement by insertion of β -glucuronidase into the viral polyprotein. *Proc Natl Acad Sci USA* **89**: 10208–10212
- Engler C, Gruetzner R, Kandzia R, Marillonnet S** (2009) Golden gate shuffling: a one-pot DNA shuffling method based on type II restriction enzymes. *PLoS ONE* **4**: e5553
- Espley RV, Hellens RP, Putterill J, Stevenson DE, Kutty-Amma S, Allan AC** (2007) Red colouration in apple fruit is due to the activity of the MYB transcription factor, MdMYB10. *Plant J* **49**: 414–427
- Fu DQ, Zhu BZ, Zhu HL, Jiang WB, Luo YB** (2005) Virus-induced gene silencing in tomato fruit. *Plant J* **43**: 299–308
- Gutha LR, Casassa LF, Harbertson JF, Naidu RA** (2010) Modulation of flavonoid biosynthetic pathway genes and anthocyanins due to virus infection in grapevine (*Vitis vinifera* L.) leaves. *BMC Plant Biol* **10**: 187
- He Q, Shen Y, Wang M, Huang M, Yang R, Zhu S, Wang L, Xu Y, Wu R** (2011) Natural variation in petal color in *Lycoris longituba* revealed by anthocyanin components. *PLoS ONE* **6**: e22098
- Hichri I, Barrieu F, Bogs J, Kappel C, Delrot S, Lauvegeat V** (2011) Recent advances in the transcriptional regulation of the flavonoid biosynthetic pathway. *J Exp Bot* **62**: 2465–2483
- Juárez P, Presa S, Espí J, Pineda B, Antón MT, Moreno V, Buesa J, Granell A, Orzaez D** (November 10, 2011) Neutralizing antibodies against rotavirus produced in transgenically labelled purple tomatoes. *Plant Biotechnol J* <http://dx.doi.org/10.1111/j.1467-7652.2011.00666.x>
- Kasschau KD, Cronin S, Carrington JC** (1997) Genome amplification and long-distance movement functions associated with the central domain of tobacco etch potyvirus helper component-proteinase. *Virology* **228**: 251–262
- Kelloniemi J, Mäkinen K, Valkonen JP** (2008) Three heterologous proteins simultaneously expressed from a chimeric potyvirus: infectivity, stability and the correlation of genome and virion lengths. *Virus Res* **135**: 282–291
- Kortstee AJ, Khan SA, Helderman C, Trindade LM, Wu Y, Visser RG, Brendolise C, Allan A, Schouten HJ, Jacobsen E** (2011) Anthocyanin production as a potential visual selection marker during plant transformation. *Transgenic Res* **20**: 1253–1264
- Lalonde S, Ehrhardt DW, Loqué D, Chen J, Rhee SY, Frommer WB** (2008) Molecular and cellular approaches for the detection of protein-protein interactions: latest techniques and current limitations. *Plant J* **53**: 610–635
- Lin-Wang K, Bolitho K, Grafton K, Kortstee A, Karunairatnam S, McGhie TK, Espley RV, Hellens RP, Allan AC** (2010) An R2R3 MYB transcription factor associated with regulation of the anthocyanin biosynthetic pathway in Rosaceae. *BMC Plant Biol* **10**: 50
- Liu Y, Schiff M, Dinesh-Kumar SP** (2002) Virus-induced gene silencing in tomato. *Plant J* **31**: 777–786
- Lu R, Malcuit I, Moffett P, Ruiz MT, Peart J, Wu AJ, Rathjen JP, Bendahmane A, Day L, Baulcombe DC** (2003) High throughput virus-induced gene silencing implicates heat shock protein 90 in plant disease resistance. *EMBO J* **22**: 5690–5699
- Luo J, Butelli E, Hill L, Parr A, Niggeweg R, Bailey P, Weisshaar B, Martin C** (2008) AtMYB12 regulates caffeoyl quinic acid and flavonol synthesis in tomato: Expression in fruit results in very high levels of both types of polyphenol. *Plant J* **56**: 316–326
- Martin K, Kopperud K, Chakrabarty R, Banerjee R, Brooks R, Goodin MM** (2009) Transient expression in *Nicotiana benthamiana* fluorescent marker lines provides enhanced definition of protein localization, movement and interactions *in planta*. *Plant J* **59**: 150–162
- Martínez F, Sardanyés J, Elena SF, Daròs JA** (2011) Dynamics of a plant RNA virus intracellular accumulation: stamping machine *vs.* geometric replication. *Genetics* **188**: 637–646
- Mathews H, Clendennan SK, Caldwell CG, Liu XL, Connors K, Matheis N, Schuster DK, Menasco DJ, Wagoner W, Lightner J, et al** (2003) Activation tagging in tomato identifies a transcriptional regulator of anthocyanin biosynthesis, modification, and transport. *Plant Cell* **15**: 1689–1703
- Orzaez D, Medina A, Torre S, Fernández-Moreno JP, Rambla JL, Fernández-Del-Carmen A, Butelli E, Martin C, Granell A** (2009) A visual reporter system for virus-induced gene silencing in tomato fruit based on anthocyanin accumulation. *Plant Physiol* **150**: 1122–1134
- Orzaez D, Mirabel S, Wieland WH, Granell A** (2006) Agroinjection of tomato fruits. A tool for rapid functional analysis of transgenes directly in fruit. *Plant Physiol* **140**: 3–11
- Ougham HJ, Morris P, Thomas H** (2005) The colors of autumn leaves as symptoms of cellular recycling and defenses against environmental stresses. *Curr Top Dev Biol* **66**: 135–160
- Piazza P, Procissi A, Jenkins GI, Tonelli C** (2002) Members of the c1/p11 regulatory gene family mediate the response of maize aleurone and mesocotyl to different light qualities and cytokinins. *Plant Physiol* **128**: 1077–1086
- Piston DW, Kremers GJ** (2007) Fluorescent protein FRET: the good, the bad and the ugly. *Trends Biochem Sci* **32**: 407–414
- Scholthof HB, Morris TJ, Jackson AO** (1993) The capsid protein gene of tomato bushy stunt virus is dispensable for systemic movement and can be replaced for localized expression of foreign genes. *Mol Plant Microbe Interact* **6**: 309–322
- Schwinn K, Venail J, Shang Y, Mackay S, Alm V, Butelli E, Oyama R, Bailey P, Davies K, Martin C** (2006) A small family of MYB-regulatory genes controls floral pigmentation intensity and patterning in the genus *Antirrhinum*. *Plant Cell* **18**: 831–851
- Thole V, Worland B, Snape JW, Vain P** (2007) The pCLEAN dual binary vector system for *Agrobacterium*-mediated plant transformation. *Plant Physiol* **145**: 1211–1219
- Tilsner J, Oparka KJ** (2010) Tracking the green invaders: advances in imaging virus infection in plants. *Biochem J* **430**: 21–37
- Torres-Barceló C, Daròs JA, Elena SF** (2010) Compensatory molecular evolution of HC-Pro, an RNA-silencing suppressor from a plant RNA virus. *Mol Biol Evol* **27**: 543–551
- Torres-Barceló C, Martín S, Daròs JA, Elena SF** (2008) From hypo- to hyper-suppression: effect of amino acid substitutions on the RNA-silencing suppressor activity of the *Tobacco etch potyvirus* HC-Pro. *Genetics* **180**: 1039–1049
- Ververidis F, Trantas E, Douglas C, Vollmer G, Kretschmar G, Panopoulos N** (2007) Biotechnology of flavonoids and other phenylpropanoid-derived natural products. Part II: Reconstruction of multienzyme pathways in plants and microbes. *Biotechnol J* **2**: 1235–1249
- Wei T, Huang TS, McNeil J, Laliberté JF, Hong J, Nelson RS, Wang A** (2010a) Sequential recruitment of the endoplasmic reticulum and chloroplasts for plant potyvirus replication. *J Virol* **84**: 799–809
- Wei T, Zhang C, Hong J, Xiong R, Kasschau KD, Zhou X, Carrington JC, Wang A** (2010b) Formation of complexes at plasmodesmata for potyvirus intercellular movement is mediated by the viral protein P3N-PIPO. *PLoS Pathog* **6**: e1000962
- Winfield C, Davies K, Gould K** (2009) Anthocyanins. Springer, New York.